Increased Amounts of HMG-CoA Reductase Induce "Karmellae": A Proliferation of Stacked Membrane Pairs Surrounding the Yeast Nucleus

Robin Wright, Michael Basson, Linda D'Ari, and Jasper Rine

Department of Biochemistry, University of California, Berkeley, California 94720

Abstract. Overproduction of the enzyme 3-hydroxy-3-methylglutaryl coenzyme A (HMG-CoA) reductase in yeast resulted in striking morphological effects on the structure of intracellular membranes. Specifically, stacks of paired membranes closely associated with the nuclear envelope were observed in strains that overproduced the HMG1 isozyme, one of two isozymes for HMG-CoA reductase in yeast. These nuclear-associated, paired membranes have been named "karmellae." In strains that overproduced the HMG1 isozyme, HMG-CoA reductase was present in the karmellar layers. At mitosis, karmellae were asymmetrically segregated: the mother cells inherited all of the karmellae and the daughter cells inherited none. A membranous structure of different morphology was occasionally found in cells that overproduced the HMG2 isozyme. These observations further establish the existence of cellular mechanisms that monitor the levels of membrane proteins and compensate for changes in these levels by inducing synthesis of particular types of membrane.

THE diverse structures and functions of biological membranes are direct consequences of their specific lipid and protein composition. Therefore, membrane biogenesis must involve temporal and spatial coordination of the synthesis and assembly of the various membrane components. An example of this coordination is the dramatic alteration of membrane structure caused by overproduction of specific membrane proteins. For example, in *Escherichia coli*, overproduction of two different membrane protein complexes, ATP synthase and fumarate reductase, leads to the formation of intracellular membrane tubules and cisternae, synthesized to accommodate the increased levels of these membrane proteins (von Meyenberg et al., 1984; Weiner et al., 1984). These studies indicate that prokaryotic cells are able to monitor the levels of individual membrane proteins and, when necessary, make compensatory changes in membrane synthesis. Eukaryotic cells also respond to increased levels of membrane proteins by increasing membrane synthesis. Induction of the endoplasmic reticulum-associated cytochrome P_{450} hydroxylases in the hepatocytes of phenobarbital-treated rats is accompanied by proliferation of the endoplasmic reticulum (ER)[1] (Jones and Fawcett, 1966; Bolender and Weibel, 1973).

The most extensive analysis of the link between the overproduction of a specific membrane protein and membrane assembly involves mammalian 3-hydroxy-3-methylglutaryl coenzyme A (HMG-CoA) reductase. HMG-CoA reductase catalyzes the rate-limiting step in sterol biosynthesis (Brown and Goldstein, 1980), and is an integral membrane protein of the ER (Brown and Simoni, 1984; Liscum et al., 1985). In mammalian cells, HMG-CoA reductase is anchored in the ER by seven membrane-spanning domains in the amino-terminal one-third of the protein (Liscum et al., 1985). In addition to its role as a membrane anchor, the membrane-bound domain is required for the regulation of HMG-CoA reductase half-life in response to sterols (Gil et al., 1985). The catalytic domain is located in the carboxyl-terminal two-thirds of the protein (Liscum et al., 1985).

In the Chinese hamster ovary-derived cell line, UT-1, synthesis of HMG-CoA reductase can be induced >500-fold above that of the parental cell line (Chin et al., 1982). Concomitant with enzyme overproduction, UT-1 cells assemble HMG-CoA reductase–containing, ER-like tubules organized in a characteristic hexagonal array known as the crystalloid ER (Anderson et al., 1983; Orci et al., 1984). Overproduction of a truncated protein containing only the catalytic domain results in elevated levels of enzyme activity without crystalloid ER formation, demonstrating that the membrane-bound domain of HMG-CoA reductase is essential for formation of crystalloid ER and that the membrane proliferation is not a consequence of increased HMG-CoA reductase activity (Jingami et al., 1987). Kinetic studies of crystalloid ER formation indicate that HMG-CoA reductase is first inserted into the outer nuclear membrane (Pathak et al., 1986). In response to continued overproduction, folds of membrane

1. *Abbreviations used in this paper*: ER, endoplasmic reticulum; HMG-CoA, 3-hydroxy-3-methylglutaryl coenzyme A.

emerge to form lamellar stacks that are subsequently transformed into crystalloid ER. When the synthesis of HMG-CoA reductase is repressed after crystalloid ER formation, HMG-CoA reductase is degraded and the crystalloid ER disappears (Orci et al., 1984).

In contrast to the single gene encoding HMG-CoA reductase in mammals (Reynolds et al., 1984), two genes for HMG-CoA reductase are present in the yeast *Saccharomyces cerevisiae* (Basson et al., 1986). Gene disruption experiments have shown that expression of either gene is sufficient for both vegetative cell growth and spore germination, but at least one functional gene is essential for viability in the absence of high levels of mevalonate, the product of the reaction catalyzed by HMG-CoA reductase. These genes, *HMG1* and *HMG2*, encode isozymes of HMG-CoA reductase with virtually identical catalytic domains (Basson et al., 1986). Secondary structure predictions based on DNA sequence analysis indicate that, as in the mammalian protein, the amino-terminal region of each yeast isozyme contains seven membrane-spanning domains (Basson, M., M. Thorsness, and J. Rine, unpublished results). However, the sequences of the transmembrane regions encoded by *HMG1* and *HMG2* have diverged extensively. This divergence may reflect a difference in the regulation or the subcellular localization of the two isozymes.

The subject of this study is an ultrastructural evaluation of the consequences of overproduction of the two yeast HMG-CoA reductase isozymes. Specifically, our results demonstrated the assembly of a novel membrane structure ("karmellae") in response to overproduction of HMG-CoA reductase encoded by *HMG1*. In contrast, a membrane structure that differed qualitatively from either karmellae or crystalloid ER was observed upon overproduction of the HMG2 isozyme. These studies reinforce previous observations that membrane protein overproduction can elicit proliferation of specialized membranes.

Materials and Methods

Strains and Culture Conditions

Table I describes the strains used in these studies. JRY527 (alias YM256) and plasmid pBM150 were obtained from M. Johnston (Johnston and Davis, 1984). JRY540 is a *cir°* strain from A. Brake (Chiron Corp., Emeryville, CA) and was derived from JRY188 (alias HR148-7C; from R. Jensen, University of California, San Diego). To place the *HMG2* gene on a multicopy yeast plasmid, the 4.9-kb Eco RI fragment containing *HMG2* from pJR322 (Basson et al., 1986) was inserted into the Eco RI site of pSEY8 (Emr et al., 1986), generating the plasmid pJR360. To increase the gene dosage of *HMG1*, the very high copy number plasmid, pC1/1 was used (A. Brake, Chiron Corp.). This plasmid is maintained at ~80 copies per cell in a *cir°* strain. The 277-bp Bam HI-Sal I fragment derived from pBR322 (Bolivar et al., 1977) is present on both pC1/1 and the *HMG1*-containing, 8.0-kb Sal I fragment from pJR59 (Basson et al., 1986). The following procedure was used to remove this Bam HI-Sal I fragment from pC1/1 before ligation to the *HMG1*-containing Sal I fragment: pC1/1, which contains unique Bam HI and Sal I sites, was digested with Bam HI. The resulting 11.9-kb linear molecule was treated with the Klenow fragment of DNA polymerase I to make the 5' extensions blunt; Sal I oligonucleotide linkers were ligated onto the ends; and the resulting molecule was digested with Sal I. The resulting 11.6-kb fragment lacking the pBR322-derived 277-bp Sal I fragment was then ligated to the 8.0-kb Sal I fragment containing *HMG1* from pJR59, generating the plasmid pJR243. All in vitro plasmid manipulations were performed as described (Maniatis et al., 1982). All plasmids were grown in the *E. coli* strain, DH-1 (Hanahan, 1983). Disrupted alleles of *HMG1* and *HMG2* were generated by insertion of the *LYS2* and *HIS3* genes, respectively (described in Basson et al., 1986).

Table I. Descriptions of Strains Used in This Study

Strain	Description
JRY527	a *HMG1 HMG2 ura3-52 his3Δ200 ade2-101 lys2-801 met*
JRY540	α *sir3-8^{ts} ura3-52 leu2$^-$ trp1^{am} his4^{am} cir°*
JRY1238	JRY527 + YEp24 (*URA3 2μ*)
JRY1239	JRY527 + pJR59 (*HMG1 URA3 2μ*; YEp24 derivative)
JRY1242	JRY527 + pJR435 (p*GAL1::HMG1 URA3 ARS1 CEN4*; pBM150 derivative)
JRY1266	a *hmg1::LYS2 HMG2 ura3-52 his3Δ200 ade2-101 lys2-801 met* + pJR360 (*HMG2 URA3 2μ*; pSEY8 derivative)
JRY1268	a *HMG1 hmg2::HIS3 ura3-52 his3Δ200 ade2-101 lys2-801 met* + pJR59 (*HMG1 URA3 2μ*; YEp24 derivative)
JRY1597	a *hmg1::LYS2 hmg2::HIS3 ura3-52 his3Δ200 ade2-101 lys2-801 met*
JRY1688	JRY540 + pJR243 (*HMG1 LEU2-d 2μ*; pC1/1 derivative)

Yeast rich medium contained 1% yeast extract, 2% Bacto-Peptone (Difco Laboratories, Inc., Detroit, MI), and 2% glucose. Yeast minimal medium consisted of 0.17% yeast nitrogen base without amino acids or ammonium sulfate (Difco Laboratories, Inc.), 5% ammonium sulfate, and 2% glucose (or 2% galactose). For solid medium, agar (Difco Laboratories, Inc.) was added to 2% final concentration. Minimal medium was supplemented with appropriate amino acids and bases at 30 mg/liter. JRY1597 (*hmg1 hmg2*) was grown in minimal medium supplemented with DL-mevalonolactone (Sigma Chemical Co., St. Louis, MO) at a final concentration of 5 g/liter.

Materials and Formulas

Glutaraldehyde and osmium were obtained from Polysciences Inc. (Warrington, PA). Potassium ferricyanide was obtained from Mallinckrodt (St. Louis, MO). Cacodylate buffer was adjusted to pH 6.8 with sodium hydroxide, and consisted of 0.1 M sodium cacodylate, 1 mM calcium chloride, and 1 mM magnesium chloride. Spurr's resin contained 10 g 4-vinylcyclohexene, 6 g DER-736, 26 g nonenylsuccinic anhydride, and 0.4 g dimethylaminoethanol (Spurr, 1969). PBS contained 140 mM sodium chloride, 3 mM potassium chloride, 8 mM dibasic sodium phosphate, and 1.5 mM monobasic potassium phosphate. PBS-Tween20 was PBS with a final concentration of 0.05% polyoxyethylene-sorbitan monolaurate. Colloidal gold was prepared and conjugated to protein A by the method of Frens, as outlined by Roth (Roth, 1982). Goat anti-rabbit IgG conjugated to colloidal gold was purchased from E. Y. Laboratories, Inc. (San Mateo, CA). 15 nM gold particles were used for all immunolabeling experiments presented here.

Electron Microscopy

The fixation protocol was adapted from that described by McDonald for mammalian cells (McDonald, 1984). Yeast cells grown to early logarithmic phase at 30°C in supplemented minimal medium were diluted into rich medium and allowed to continue growth for one to two generations. 50–100 ml of a culture containing 5 × 10^6 cells/ml produced a pellet sufficiently large for processing. The cells were harvested by centrifugation, washed twice with minimal medium, and then resuspended in minimal medium at 1/20 of the original culture volume. An equal volume of ice-cold 2× fixative (4% glutaraldehyde in 0.2 M cacodylate buffer, pH 6.8) was added rapidly to ensure uniform mixing. After incubation for 5 min at room temperature, the cells were pelleted and resuspended in 1× fixative (1/10 original culture

volume). Fixation continued on ice for 30 min. After fixation, glutaraldehyde was removed by three washes in 0.1 M cacodylate buffer, pH 6.8. The cell pellet was resuspended in a freshly mixed, ice-cold solution of 0.5% osmium tetroxide and 0.8% potassium ferricyanide in 0.1 M cacodylate buffer, pH 6.8 (1/50 original culture volume). The cells were incubated on ice as a suspension for 5 min and then centrifuged for 5 min at room temperature in a clinical centrifuge. The postfixative was replaced with an equal volume of newly mixed postfixative, taking care not to disturb the pellet. Postfixation was continued for 15 min on ice after which the pellet was washed three times in distilled water and en bloc stained in 2% aqueous uranyl acetate for 1 h at room temperature. In some experiments, staining occurred overnight at 4°C. Cells were then dehydrated through a graded ethanol series and embedded in Spurr's resin. After polymerization overnight at 60°C, silver-to-gold sections (~90 nM thick) were cut using a diamond knife and mounted on 200-mesh nickel or copper grids. For serial sections, the leading and trailing edge of the block-face were coated with diluted rubber cement (Fahrenbach, 1984) and the ribbons were picked up onto formvar-coated slot grids. Sections were stained with Millonig's lead tartrate (as described in Hayat, 1981) for 10–20 min. Observations were made on a Philips 301 microscope at 80 kV. Micrographs were printed on Agfa Broviraspeed paper, contrast grades 2 and 3.

Immunoelectron Microscopy

Sections of cells prepared as above were mounted on 200-mesh nickel grids with formvar-coated bars. To ensure retention of sections, the grids were subsequently heated at 60°C for 2–5 min. Sections prepared in this manner have shown no loss of staining capacity or resolution over a period of 3 mo. For immunostaining, the grids were immersed in blocker (1% ovalbumin in PBS-Tween 20) at room temperature for 15 min and then placed directly into antiserum that had been diluted in blocker to a concentration of ~20 μg of IgG per ml. After a 2-h incubation at room temperature, the grids were washed by sequential transfer through five changes of PBS-Tween20 and then immersed in the gold-labeled secondary serum for 1 h at room temperature. Protein A and goat anti-rabbit IgG gold conjugates gave similar results, although the immunoglobulin preparation produced slightly less nonspecific background staining. The grids were then washed as above, followed by a final rinse in distilled water. Sections were then poststained and observed as described above.

Antisera Preparation and Characterization

A hybrid protein in which the catalytic domain of the HMG1 protein was fused to the carboxyl terminus of *E. coli* β-galactosidase was prepared as follows. A 1.73-kb Eco RI fragment containing the 3′ half of the *HMG1* coding region from pJR59 (Rine et al., 1983; Basson et al., 1986) was isolated and the 5′ extensions were made flush with DNA polymerase I Klenow fragment. The fragment was ligated into pUR288 (Ruther and Muller-Hill, 1983) which had been cleaved with Xba I and the 5′ extensions made flush with DNA polymerase I Klenow fragment, thus generating pJR349. When induced with isopropyl-β-D-thiogalactopyranoside (Sigma Chemical Co.), the *E. coli* strain BMH71-18 (Messing et al., 1977) carrying pJR349 produced a β-galactosidase-HMG1 fusion protein of ~169 kd containing amino acids 523–1,054 of the HMG1 protein. The fusion protein was purified by SDS gel electrophoresis and injected into rabbits. Crude serum was purified using an affinity column containing the antigen coupled to Sepharose 4B (Pharmacia, Inc., Piscataway, NJ). Bound antibodies were eluted from the column with 0.2 M glycine, pH 2.5, immediately neutralized with 3 M Tris-HCl, pH 9, and stored in aliquots at −20°C. Because of the extensive similarity between the carboxyl-terminal halves of the HMG1 and HMG2 proteins, the serum recognized both proteins on immunoblots. The affinity-purified serum was used at a concentration of ~20 μg IgG per ml for immunolabeling and at 2 μg IgG per ml for immunoblots. The method described by Burnette was followed for detection of HMG-CoA reductase by immunoblotting (Burnette, 1981).

Results

Karmellae Are Paired Bilayers That Assemble in Stacks Around the Nuclei of Cells That Overproduce HMG-CoA Reductase

We initially examined the ultrastructure of yeast cells that overproduced HMG-CoA reductase as a result of the increased gene dosage conferred by multicopy plasmid vectors. *HMG1 HMG2* strains carrying either the multicopy plasmid pJR59 containing *HMG1* (JRY1239) or the plasmid vector with no insert (JRY1238) were compared. The increased gene dosage of *HMG1* conferred by pJR59 results in ~10-fold overproduction of both HMG-CoA reductase activity (Rine et al., 1986) and protein (see Fig. 6).

An ultrastructural abnormality was immediately apparent in the strain overproducing the HMG1 isozyme. Approximately 35% of these cells displayed a membrane proliferation consisting of nuclear-associated stacks of paired membranes. We refer to these additional paired membranes as "karmellae" to emphasize both their nuclear association (kar from the Greek root for nucleus) and their stacked appearance (mellae from an abbreviation of lamellae). The electron micrographs in Fig. 1 illustrate examples of karmellae in this strain. Each layer of karmellae consisted of a closely apposed pair of membranes, morphologically identical to the normal double membrane of the nuclear envelope. In Fig. 1 *B*, the organization of karmellae as pairs of membranes is apparent since both leaflets of each membrane bilayer in the karmellar stacks are well resolved at this magnification. The spacing and organization of the layers were typically very uniform and regular, as shown in Fig. 1 *B*, but occasionally the layers appeared more closely apposed or exhibited small discontinuities. Ribosomes and other cytoplasmic components were excluded from the area between adjacent layers of karmellae.

Karmellae appeared similar to the membrane proliferation observed in UT-1 cells at early times after induction of HMG-CoA reductase overproduction. However, a mature crystalloid ER membrane arrangement, typified by hexagonal arrays of smooth membrane tubules and characteristic of the UT-1 cells at later times after induction, was never observed in any yeast strain examined. Even when karmellae extended into the cytoplasm (see below), they were found in sheets or layers and never as tubular elements.

The Number of Karmellae per Nucleus Was Limited to 10 or Fewer

The number of karmellae per nucleus varied from as few as one (i.e., a nucleus with an inner and outer nuclear membrane plus an additional pair of membranes) to as many as 10. The distribution of karmellae per nucleus in a population of cells overproducing the HMG1 isozyme was determined from micrographs of randomly chosen cells (Fig. 2). Nuclei generally had five or fewer karmellae and no bias was observed toward either odd or even numbers or a preferred number of karmellae. Nuclei with 9 or 10 karmellae were uncommon (3 out of 98 karmellae-containing cells scored). In addition, no cell with >10 karmellae was found in at least 400 additional karmellae-containing cells that were observed but not photographed.

To minimize variations in the level of *HMG1* overexpression due to differences in plasmid copy number per cell, the complete *HMG1* open reading frame was fused to the strong, inducible *GAL1* promoter and placed on a centromere-containing plasmid, producing plasmid pJR435 (Basson, M., and J. Rine, unpublished results). The centromere sequences maintain plasmid copy number at one or two per cell (Clarke

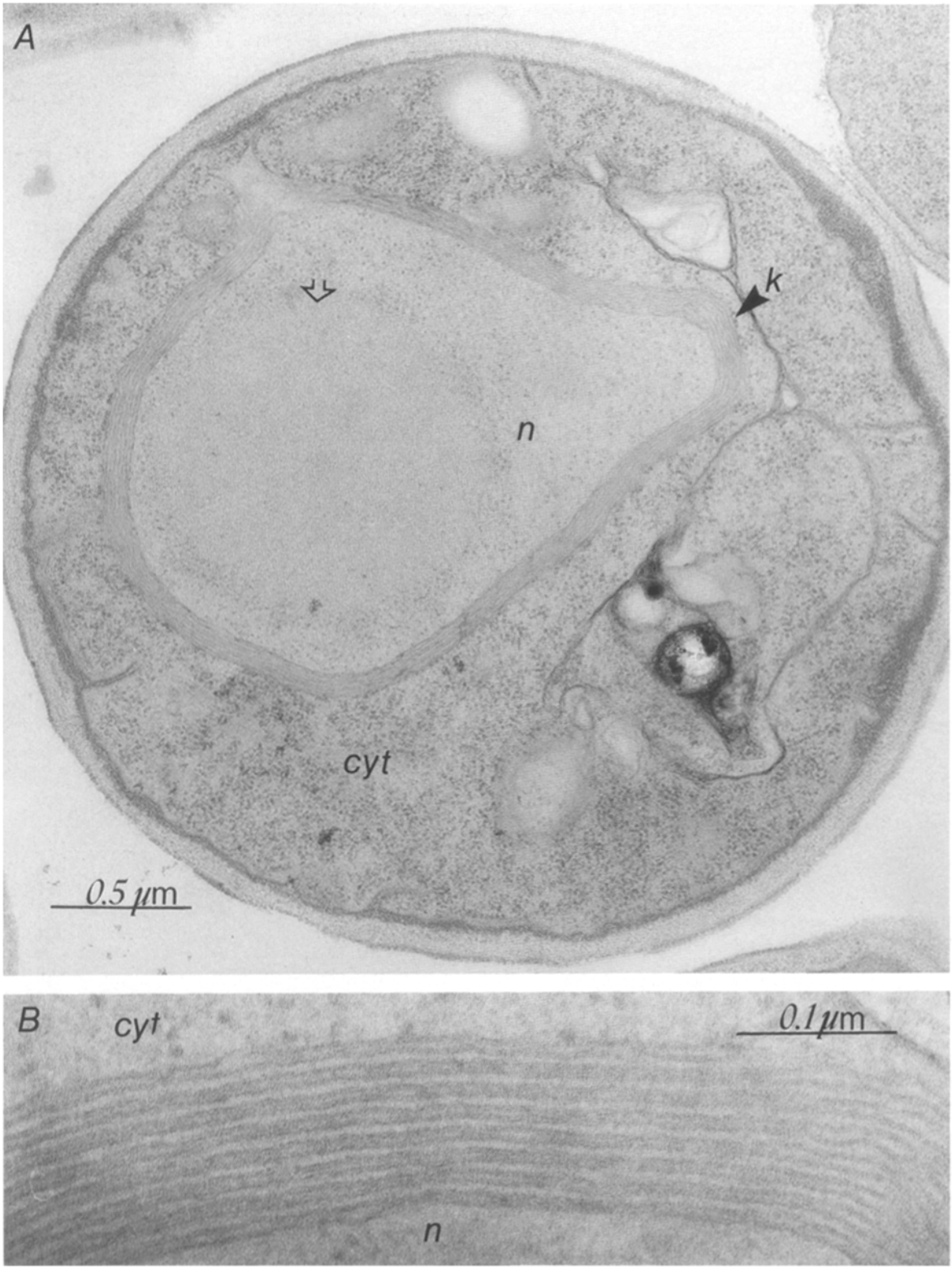

Figure 1. Karmellae are paired membranes that assemble in stacks around the nucleus of yeast cells that overproduce the HMG1 isozyme of HMG-CoA reductase. *A* shows an electron micrograph of a section through an entire karmellae-containing cell (JRY1239). The small open arrowhead points to the zone of unusual staining density seen in the nucleoplasm of karmellae-containing cells. Normal ER, situated just beneath the plasma membrane, is also apparent in this cell. *B* is a higher magnification of karmellar layers from another JRY1239 cell. The bilayers of each membrane in the stack are well resolved and the organization of karmellae as pairs of membranes is clearly apparent. *cyt*, cytoplasm; *k*, karmellae; *n*, nucleus.

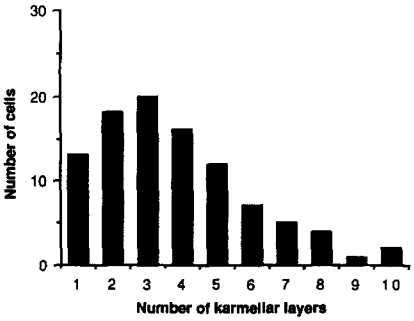

Figure 2. The number of karmellae per nucleus in a strain that overproduced the HMG1 isozyme 10-fold varied from 1 to 10. Electron micrographs of 98 karmellae-containing cells in a JRY1239 population were examined and the number of karmellar layers per nucleus was scored. For this analysis, cells in the population that did not contain karmellae were not considered. The distribution of the number of karmellae per nucleus ranged from 1 (a nuclear envelope plus one extra pair of membranes) to 10. No nucleus was observed with >10 karmellar layers.

and Carbon, 1980) and HMG1 overproduction results from induction of the highly expressed *GAL1* promoter rather than from gene dosage effects. The extent of HMG1 overproduction in cells containing the *pGAL1::HMG1* fusion when grown on galactose-containing medium was similar to that observed in cells containing pJR59 and these cells also contained karmellae. Although the number of karmellar layers did not increase when *HMG1* was expressed from the *GAL1* promoter, karmellae were present in a greater fraction of the cells: karmellae were found in 55% of sections through nuclei carrying the *pGAL1::HMG1* plasmid and in 35% of the nuclear sections in the strain carrying the multi-copy plasmid (pJR59). Centromere-containing plasmids are more uniformly transmitted to daughter cells at mitosis than plasmids that lack such sequences (Clarke and Carbon, 1980). Thus, the difference in the percentage of cells with karmellae due to gene dosage versus induced expression probably reflects the lower mitotic stability of the multicopy plasmid pJR59 as compared to the centromere-containing plasmid pJR435, although this was not directly examined.

Upon growth in galactose-containing medium, cells containing the *pGAL1::HMG1* plasmid express *HMG1* from the *GAL1* promoter and 5′-untranslated leader sequence. It is unlikely that normal feedback repression of HMG-CoA reductase synthesis can be exerted on this promoter-fusion gene or the resulting message, yet these cells accumulated no more than 10 layers of karmellae, similar to cells with the multicopy plasmid. Consequently, it may be that the limit in the number of karmellar layers is due to active turnover of karmellae rather than to direct regulation of gene expression. This possibility was supported by observations of cells containing the *HMG1* gene in pJR243, a plasmid that is present in ~80 copies per cell, rather than the 10 copies per cell characteristic of pJR59. These cells also showed no increase in the average number of karmellar layers. However, the vacuole, equivalent to the lysosome of animal cells, frequently contained karmellae-like membrane stacks (data not shown). Such membranes were never observed in the vacuoles of cells that expressed lower levels of HMG-CoA reductase (i.e., cells containing pJR59 or pJR435) nor in control cells that expressed a wild-type level of HMG-CoA reductase.

Karmellae Did Not Completely Encompass the Nuclei of the HMG1-overproducing Strain

In some sections, the nucleus appeared completely encased by karmellae in a manner reminiscent of the layers of an onion. However, analysis of serial sections demonstrated that most, if not all, karmellae-containing nuclei also possessed a region where only the single nuclear envelope (i.e., a pair of membranes) separated nucleoplasm from cytoplasm (Fig. 3). All strains used in this study were haploid and exhibited the axial budding pattern characteristic of haploid cells. Consequently, newly forming buds and bud scars from previous divisions were clustered at one pole of the cell. In dividing cells, the akarmellar region was always oriented toward the newly forming bud. In unbudded cells, this region was often, but not invariably, oriented toward bud scars from previous divisions.

Nuclear pores were concentrated in the akarmellar region and were rarely seen in the stacks of karmellae (see Fig. 9). However, in nuclei with one or two karmellae, some pores were aligned to form a complete channel between nucleoplasm and cytoplasm through four to six membranes. This arrangement was not observed with increased numbers of karmellae.

Microtubules and spindle-pole bodies were rarely observed in our electron microscopy preparations. The osmium/potassium ferricyanide fixation was not optimal for preservation of these structures, probably due to microtubule depolymerization induced by calcium in the fixative buffer. However, in those cases in which spindle-pole bodies were unambiguously observed in karmellae-containing nuclei, they were present only in the akarmellar regions.

The innermost membrane pair of karmellar nuclei was generally inferred to be the nuclear envelope since it was usually continuous, encircling the nucleoplasm completely. However, this organization was not always observed. In some cells, the karmellar membranes and the membranes of the akarmellar region were clearly discontinuous, resulting in a two-part membrane structure surrounding the nucleus (Fig. 3). At the junctions between the two membrane regions, the innermost, nuclear-proximal double membrane and the outermost karmellar layer were sometimes continuous (Fig. 3 *C*). In other cells, the discontinuity of the innermost membrane layer appeared different (Fig. 3 *E*). In addition, multiple membrane termini or loops were associated with the nucleoplasm in a staggered arrangement in some cells (Fig. 3 *D*). Fig. 4 is a sketch which summarizes these observations.

Ribbons of Karmellae often Extended Away from the Nucleus into the Cytoplasm

Ribbons of karmellae often appeared as though they had been "peeled" away from the nucleus, extending into the cytoplasm (Fig. 5). Even in these cases, the characteristic stacked, lamellar arrangement was maintained and no conversion to a tubular organization was observed. The cytoplasmic karmellae were often associated with the plasma membrane or the vacuole, lacking any obvious nuclear association. However, examination of serial sections revealed that karmellae apparently unassociated with the nucleus at one plane of section were nuclear associated at a different level within the cell. Consequently, cytoplasmic karmellae were not separate

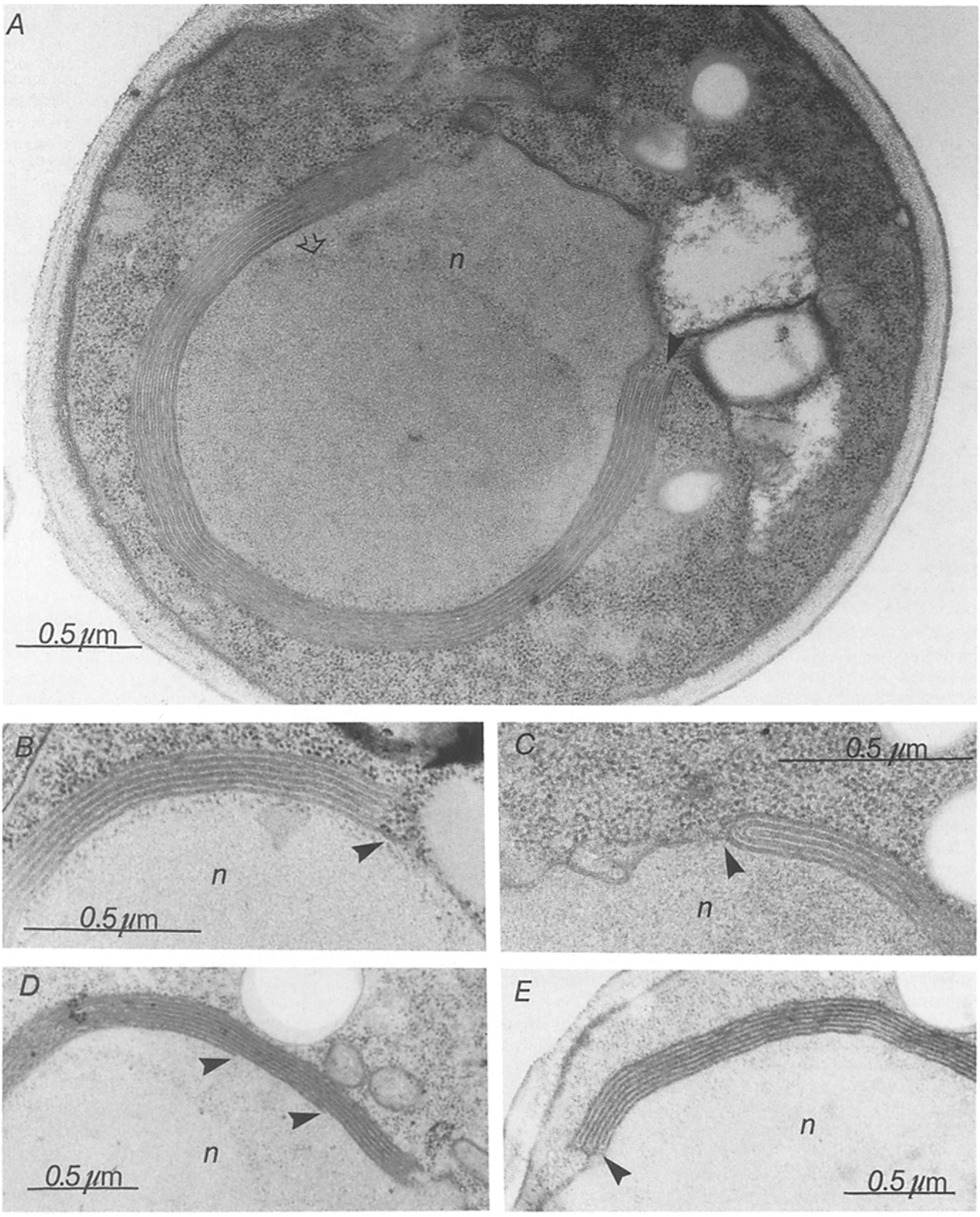

Figure 3. Karmellae did not completely encircle the nucleus, but an akarmellar region consisting of a single membrane pair was retained. The junction between the akarmellar region and the karmellar layers varied. These micrographs depict a number of variations in this junction in JRY1239 cells. *A* shows a section through an entire cell. The innermost karmellar layer and the nuclear envelope are continuous. The stacks of karmellae consist of separate folds of membrane. The small open arrowhead points to a zone of unusual stain density seen in karmellae-containing nuclei. In *B*, the innermost karmellar layer and the nuclear envelope are also continuous. In this cell, however, the

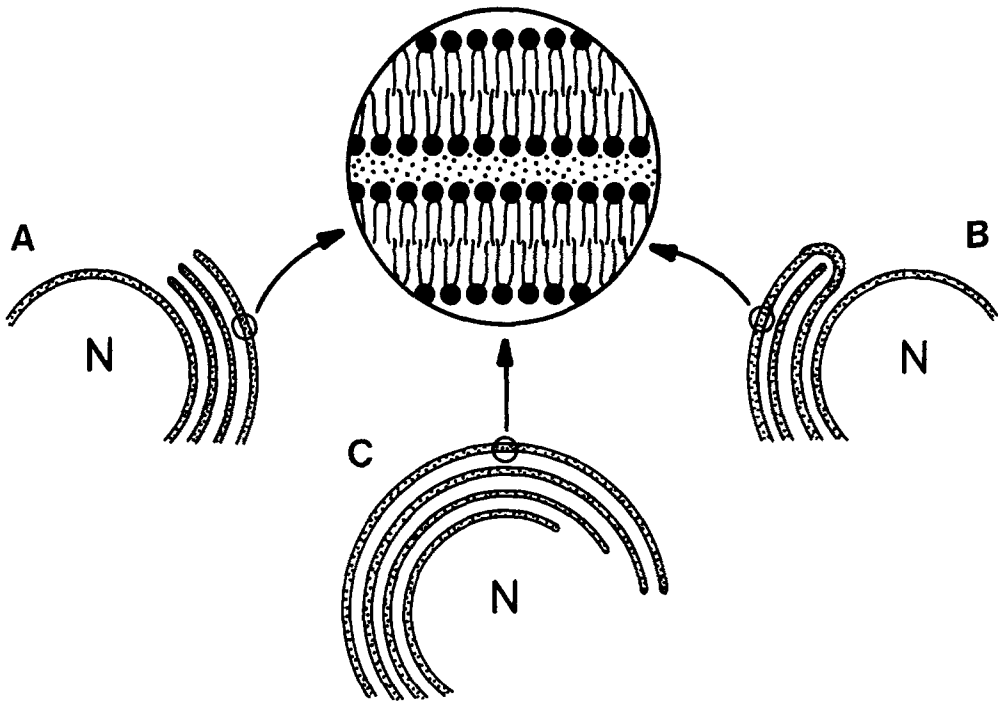

Figure 4. Karmellar layers could assemble as separate folds of membrane or in a variety of nested configurations. This sketch shows an idealized view of both the folded (*A*) and the nested (*B*) arrangements of karmellae. The distance between the pair of membranes that constitute a karmellar layer and between the membrane layers has been exaggerated for clarity. In addition, the lumen between the paired bilayers is stippled to distinguish it from the cytoplasmic space between adjacent karmellae. The nuclear envelope in *B* is drawn as if it were continuous between the akarmellar and karmellar regions, but this arrangement was not always observed (see Fig. 3, *C* and *E*). *C* depicts the staggered arrangement of the nuclear envelope seen in some karmellae-containing cells (see Fig. 3 *D*). *N*, nucleus. (Illustration by M. K. Thorsness.)

entities within the cytoplasm but, rather, were portions of karmellae that extended away from the nucleus into the cytoplasm and back to the nucleus.

HMG-CoA Reductase Is Concentrated in Karmellae

To analyze the localization of HMG-CoA reductase within the yeast cell, polyclonal antiserum was raised against a fusion protein containing the amino-terminal portion of β-galactosidase and the catalytic domain of the HMG1 protein. The resulting antiserum reacted with both the HMG1 and HMG2 isozymes on immunoblots due to the sequence similarity between the catalytic domains of the two proteins. Fig. 6 is an an immunoblot demonstrating the specificity of the affinity-purified anti-HMG-CoA reductase serum as well as the relative amounts of HMG-CoA reductase protein present in the wild-type strain and in strains that overproduced the HMG1 and HMG2 isozymes.

By using this affinity-purified antiserum, the location of HMG-CoA reductase in strains with karmellae was analyzed by indirect immunoelectron microscopy. Sections of the same preparations used for the ultrastructural studies described above were incubated in the antiserum followed by incubation in gold-conjugated secondary antibodies. Gold particles marking the position of HMG-CoA reductase appeared throughout the layers of karmellae in strains that overproduced the HMG1 isozyme (Fig. 7). Control sections that were exposed to only the gold-conjugated secondary antibody showed essentially no labeling. Sections incubated in the pass-through fraction from the column used for affinity purification or in preimmune serum did not display specific labeling of karmellae as observed with anti-HMG-CoA reductase serum. These results established that HMG-CoA reductase was present in the membranes that were assembled in response to overproduction of the HMG1 isozyme.

When incubated with the affinity-purified anti-HMG-CoA reductase serum, a low density of gold particles was observed throughout the cytoplasm of strains that did not overexpress either HMG-CoA reductase isozyme (i.e., strains with the genotypes *HMG1 HMG2*, *hmg1 HMG2*, and *HMG1 hmg2*). No concentration of gold particles was seen in association with the nucleus or with any other organelle in these cells. This labeling pattern probably represents nonspecific background labeling, since it was identical to that observed in negative control experiments in which the pass-through fraction from the affinity column was used to stain HMG1-overproducing cells. This pattern was also identical to that observed when *hmg1 hmg2* cells (JRY1597), lacking both HMG-CoA reductase isozymes, were incubated with the affinity-purified anti-HMG-CoA reductase serum. Con-

karmellar layers are partially nested, rather than distinctly separate folds of membrane. *C* shows a nested configuration of karmellar layers. In this instance, the membranes of the akarmellar region and the karmellar membranes are separate. As indicated by the arrowhead, it is apparent that the nuclear envelope and the outermost karmellar layer are continuous, producing an extreme example of the nesting of membrane layers seen in some karmellae-containing nuclei. *D* shows a nucleus with multiple, staggered ends of the nuclear envelope (*arrowheads*). The micrograph shown in *E* also demonstrates a discontinuity between the membranes of the akarmellar region and the karmellar membranes. The karmellar layers of this cell are also nested, but in a different arrangement from those shown in *B* or *C*. *n*, nucleus.

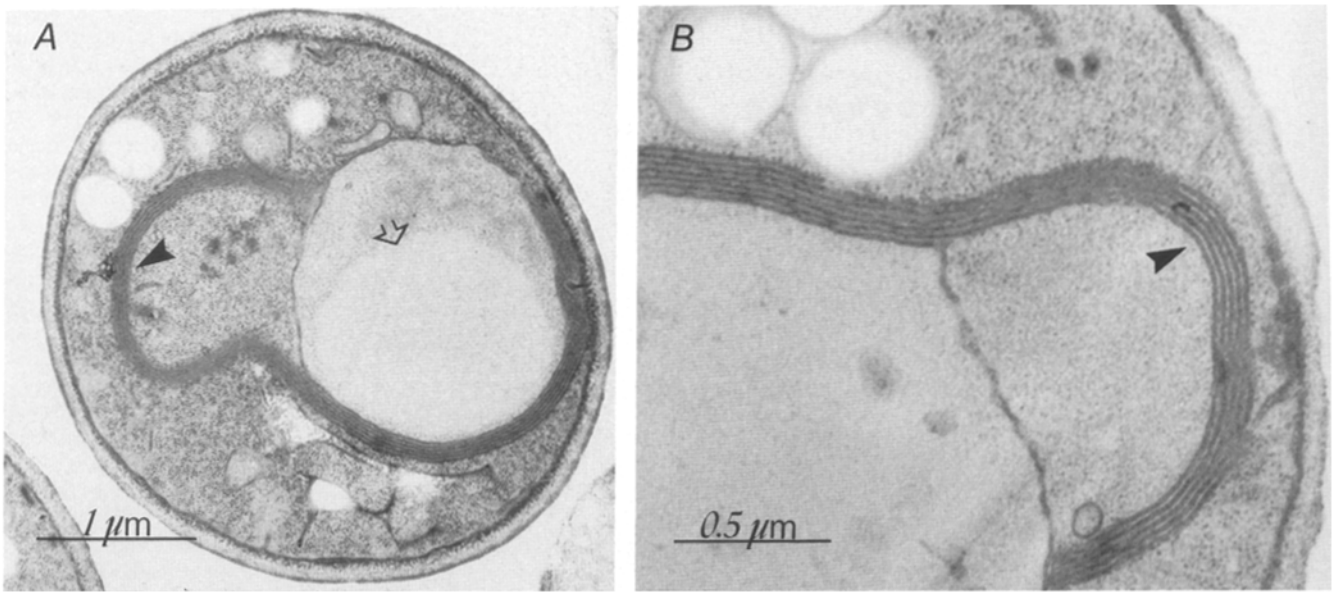

Figure 5. Ribbons of karmellae were often found in the cytoplasm. Examples of these ribbons in two different JRY1239 cells are shown in *A* and *B* (*arrowheads*). Note that the ribbons formed loops that extended away from the nucleus and then back again. Thus, ribbons of karmellae were not found as separate entities in the cytoplasm, but rather were always associated with the nucleus. Also, the characteristic stacked arrangement of karmellae was maintained even when present as ribbons that extended into the cytoplasm. The small open arrowhead marks the zone of unusual stain density seen in karmellae-containing nuclei.

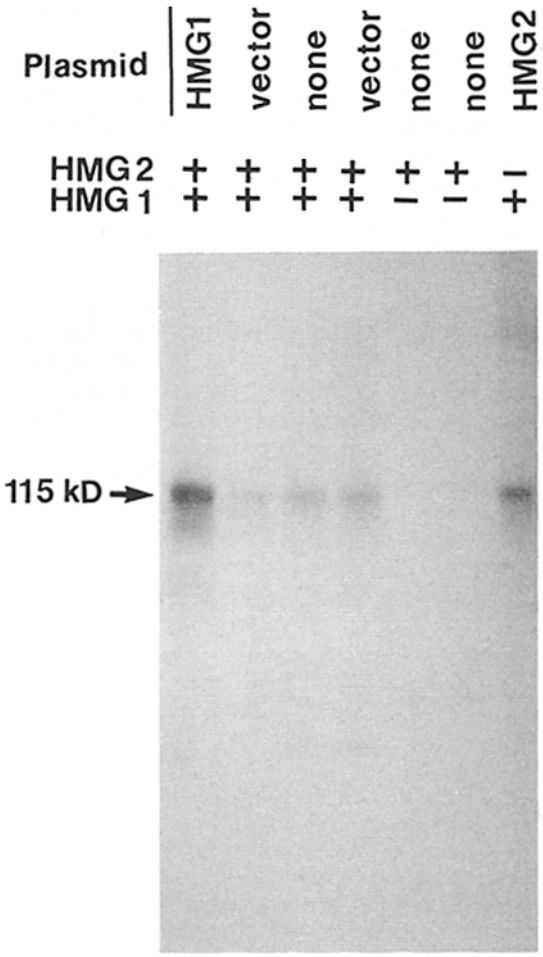

sequently, the localization of HMG-CoA reductase in strains that do not overexpress the protein could not be determined by immunoelectron microscopy.

Overproduction of the HMG2 Isozyme Did Not Result in Karmellae Formation

Strains that overproduced the *HMG1*-encoded isozyme assembled karmellae, even when the chromosomal *HMG2* gene was nonfunctional due to gene disruption. Since karmellae were formed in cells lacking a functional *HMG2* gene, an interaction between the two yeast HMG-CoA reductase isozymes was not essential for karmellae formation. To determine if overproduction of the HMG2 isozyme was also sufficient to induce karmellae assembly, the ultrastructure of an *hmg1 HMG2* strain carrying the multicopy plasmid pJR360 containing *HMG2* was also examined. Based on immunoblots using affinity-purified anti–HMG-CoA reductase

Figure 6. Affinity-purified anti–HMG-CoA reductase serum prepared against a hybrid protein containing β-galactosidase fused to the catalytic domain of the HMG1 protein recognized both HMG1 and HMG2 proteins. The plus and minus signs denote the presence or absence of functional *HMG1* or *HMG2* genes in the genome of the strain. Plasmids carried by the strain are listed at the top of each lane. Cross-reactivity of the antiserum was observed with extracts from strains that contained a disruption of either the *HMG1* or *HMG2* genes. Moreover, overproduction of either isozyme using the multicopy plasmids pJR59 (*HMG1*) or pJR360 (*HMG2*) resulted in an ~10-fold increase in signal intensity. It is difficult to directly compare the amounts of HMG-CoA reductase protein in strains that overproduced the HMG1 isozyme versus those that overproduced the HMG2 isozyme since the antiserum may not have equal affinity or avidity for the two proteins.

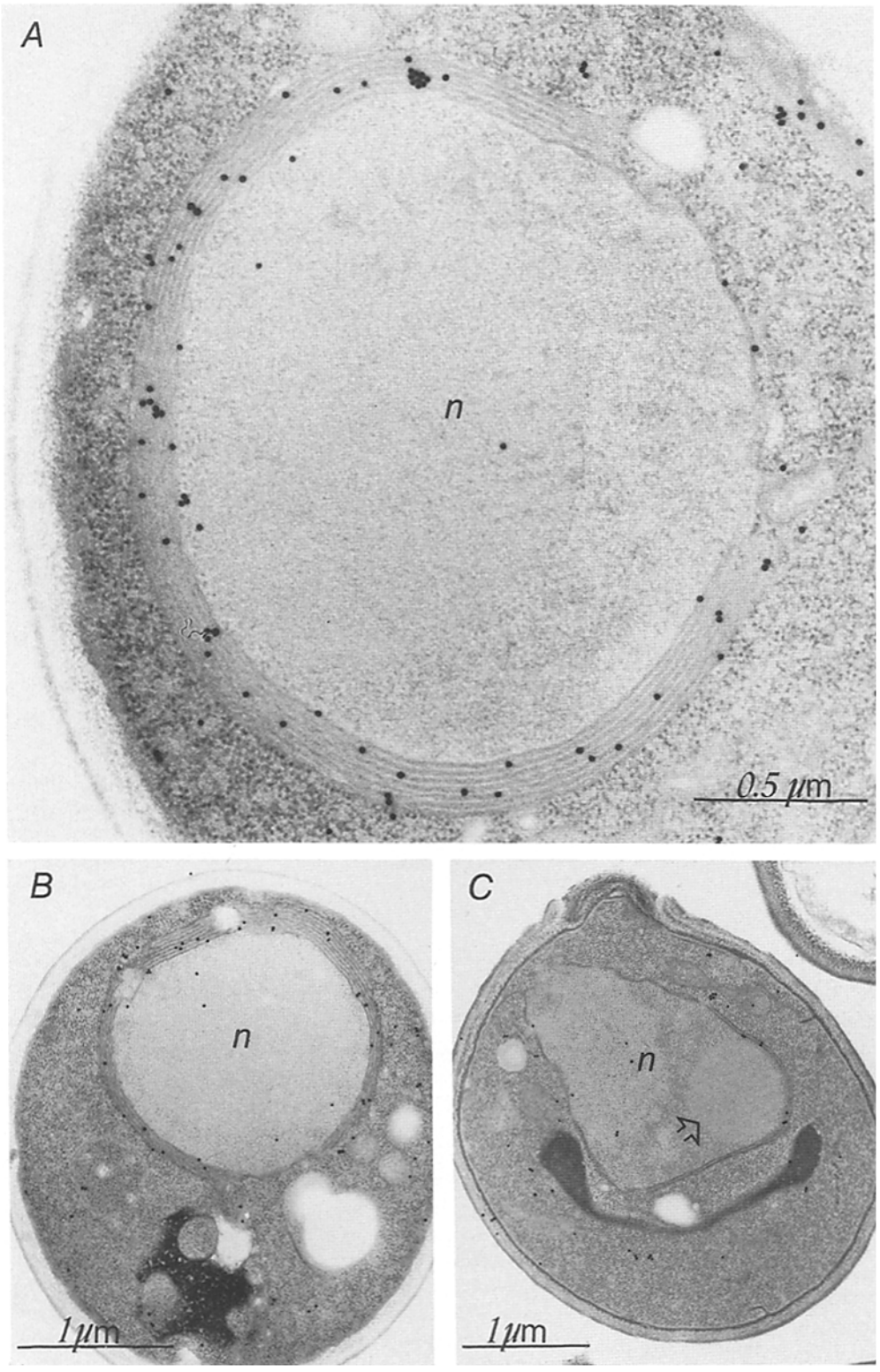

Figure 7. HMG-CoA reductase protein was present in karmellae. Sections of JRY1239 cells that overproduced the HMG1 isozyme were immunolabeled as outlined in Materials and Methods. The gold particles were concentrated in the karmellar membranes. This was especially apparent in cells with numerous karmellar layers, as shown in *A* and *B*. Cells without karmellae in the population of cells overproducing the HMG1 isozyme showed no specific labeling pattern, but gold particles were present throughout the cytoplasm in a random fashion. *C* shows a cell with only one karmellar layer; the cytoplasmic labeling is apparent as well as a low density of gold particles associated with the karmellar layer. The region of unusual staining density in the nucleus is marked with a small open arrowhead. *n*, nucleus.

serum, we estimate that HMG-CoA reductase was overproduced 10-fold above the level in the same strain lacking the plasmid (Fig. 6). It is difficult to use the immunblot data to compare the relative amounts of HMG-CoA reductase in the strains that overproduced the HMG1 isozyme versus the HMG2 isozyme, since the anti-HMG-CoA reductase serum probably does not have equal avidity or affinity for the two proteins. However, the data suggest that the amount of HMG-CoA reductase in the strain overproducing the HMG2 isozyme was considerably less than that in the strain overproducing the HMG1 isozyme.

Karmellae were never observed in the cells that overproduced the HMG2 isozyme. Most cells appeared indistinguishable from cells of either the parental strain without a

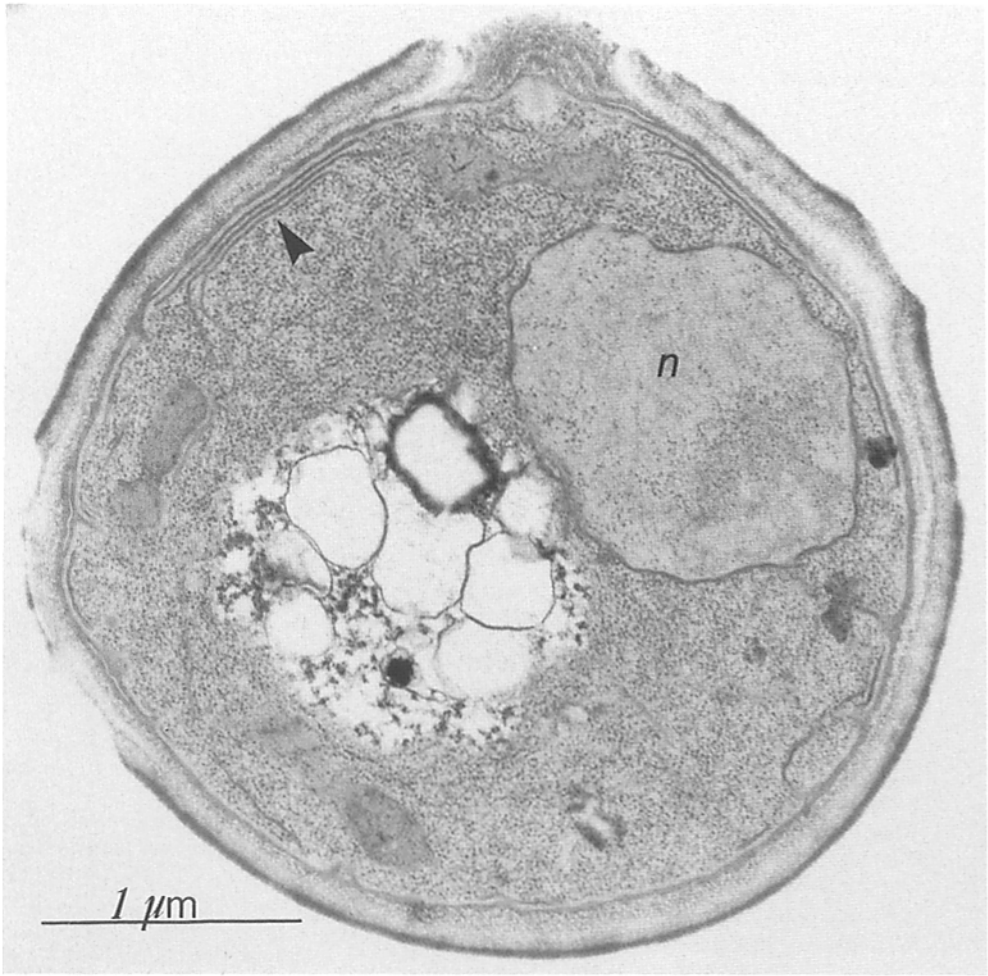

Figure 8. Karmellae were not observed in cells that overproduced the HMG2 isozyme of HMG-CoA reductase (JRY-1266). A small percentage of cells in the population contained a morphologically different form of membrane proliferation that consisted of stacks of membrane closely associated with the plasma membrane (*arrowhead*). Note the different appearance from normal, plasma membrane-associated ER (compare with Fig. 1 *A*). *n*, nucleus.

plasmid or from a congenic *HMG1 HMG2* strain. However, in the population of cells that overproduced the HMG2 isozyme, a small percentage of cells contained a qualitatively different form of membrane proliferation. This membrane structure consisted of layers of smooth ER-like, flattened membranes positioned near the plasma membrane (Fig. 8).

Cells that overproduced the HMG2 isozyme displayed no obvious pattern of staining when the localization of HMG-CoA reductase was examined by immunoelectron microscopy. Unlike the association of HMG-CoA reductase with karmellae, no concentration of gold particles was associated with the membrane proliferations that were present in the cells that overproduced the HMG2 isozyme. These results were surprising, since the antiserum reacts with both the HMG1 and HMG2 proteins in immunoblots (Fig. 6). We do not know whether the lack of staining reflects lability of the HMG2 protein during preparation for immunoelectron microscopy, interactions of the HMG2 protein with other molecules that mask antigenic determinants required for immunoreactivity, the relatively low amount of HMG-CoA reductase protein in these cells, or merely lower affinity or avidity of the antiserum for the HMG2 protein.

Karmellae Are Retained by Mother Nuclei during Mitosis

Since the expression of *HMG1* coding sequences from the *GAL1* promoter was expected to result in uniform overproduction of HMG-CoA reductase in each cell, it was surprising that only 55% of the cells in a population formed karmellae (see above). Mitosis in *S. cerevisiae* occurs by a process of budding and generates a mother cell and a daughter cell that differ in size and several other characteristics. The close correspondence between the fraction of the population that are mother cells and the fraction that contain karmellae led us to investigate karmellae segregation at mitosis.

Serial sections of karmellar nuclei undergoing mitosis revealed that karmellae were not segregated equally to mother and daughter nuclei. We distinguished mother from daughter by the presence of bud scars on the mother cell. In addition, the cell wall was often slightly thicker and the cytoplasm more densely stained in the mother cell (data not shown). Sections showing the nucleus extending into daughter cells demonstrated that karmellae remained exclusively associated with the mother nucleus (Fig. 9). Karmellae were retained around the mother cell nucleus, often extending up to the cytoplasmic bridge between the two cells. From this

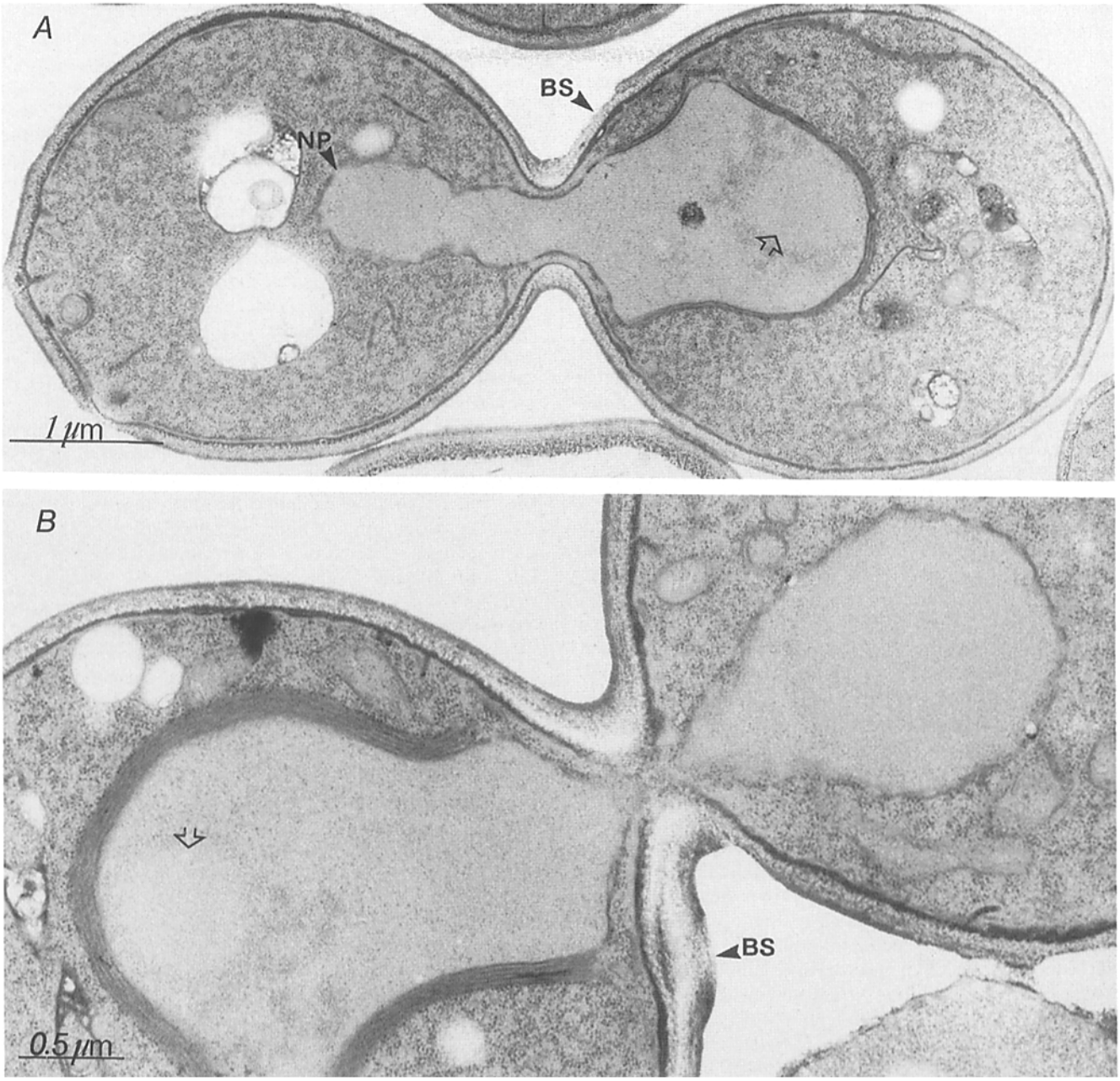

Figure 9. Karmellae were asymmetrically segregated at mitosis: the mother cell retained all karmellae and the daughter cell inherited none. These micrographs are examples of serially sectioned karmellae-containing cells (JRY1242) during mitosis. Karmellae were observed up to the cytoplasmic bridge connecting the mother and daughter cells, but from that point, only an unelaborated nuclear envelope extended into the daughter cell. Nuclear pores are readily visible in the region of normal nuclear envelope extending into the daughter cells. The small open arrowheads point to the zone of unusual staining density within the karmellae-containing nucleus. Bud scars that unambiguously identify the mother cells are marked with solid arrowheads. *BS*, bud scar; *NP*, nuclear pore.

point, a normal nuclear envelope with one double membrane extended into the daughter cell. No deviation from this asymmetric pattern of segregation was observed in serial sections of 10 mitotic cells. Furthermore, no ribbons of karmellae extended into the daughter cell, so that the daughter cell received no portions of karmellae. The maternal inheritance of karmellae was confirmed by examination of a large number of mitotic cells by immunofluorescence using affinity-purified anti–HMG-CoA reductase serum according to the method of Adams and Pringle (Adams and Pringle, 1984; data not shown).

Nuclei That Possessed Karmellae Had an Unusual Internal Ultrastructure, Apposed To the Karmellar Region of the Nucleus

Nuclei that possessed karmellae displayed an unusual internal ultrastructure close to the karmellar layers. Examples are

shown in Figs. 1 *A*, 3 *A*, 5 *A*, 7 *C*, 9, *A* and *B*, marked with small open arrowheads. This structure consisted of a spherical zone with uniform electron density positioned on one side of the nucleus. The zone was clearly distinguishable from both the chromatin-containing regions and the nucleolus of wild-type nuclei, although it was often closely associated with areas of nucleolar material. The zone could be seen in sections through regions where karmellae were continuous around the nucleus as well as in sections through the akarmellar region. Intriguingly, in longitudinal sections passing through both the karmellar stacks and the akarmellar region, the zone was always positioned opposite to the akarmellar region of the nucleus and thus nearest the karmellae. This zone of unusual staining density was observed only in karmellar nuclei and was never found in cells that did not overproduce HMG1 nor in those cells that lacked karmellae in HMG1-overproducing populations. The positioning of this structure may indicate that the proliferation of the nuclear membrane influences nucleoplasm structure.

Discussion

In yeast, overproduction of the HMG-CoA reductase isozyme encoded by HMG1 results in elaboration of a novel membrane structure that we refer to as karmellae. Karmellae consist of paired membranes arranged in layers around the nucleus and occur when the HMG1 isozyme is overproduced either by the increased gene dosage conferred by multicopy plasmid vectors or by fusion of a strong, inducible promoter to the *HMG1* coding sequences. Assembly of karmellae occurs in the presence or absence of the HMG2 isozyme and therefore does not require interactions between the two yeast isozymes. In contrast, karmellae are not assembled in cells that overproduce the HMG2 isozyme, although these cells sometimes contain membrane proliferations that are morphologically different from karmellae. Immunolocalization procedures demonstrate that HMG-CoA reductase is present in karmellar layers. Thus, it appears that overproduction of this membrane protein induces the synthesis of a membrane into which the protein is inserted and subsequently resides.

One of the more striking aspects of karmellae is that they do not inflict any notable pathology upon the cells in which they reside: strains that produce karmellae mate, sporulate, and germinate normally. Although some of these processes may be carried out by cells in the population lacking karmellae, cells containing karmellae undergo mitosis (Fig. 9) and must traverse the cell cycle at a normal rate, since these strains have a normal rate of growth. The observation that karmellae do not completely surround the nucleus may be relevant to the ability of karmellae-containing strains to perform all aspects of the yeast life cycle: all karmellae-containing nuclei appear to retain an akarmellar region where one membrane pair is the only barrier between nucleoplasm and cytoplasm. Since nuclear pores are enriched in this region, the ordinary transactions of the nuclear envelope may now be concentrated in this localized portion of the envelope. As discussed below, the akarmellar region may also be important in selection of the site of bud emergence or in the extension of the nuclear envelope into the bud.

The budding pattern of *S. cerevisiae* during mitosis allows unambiguous identification of the mother and daughter cells after each mitosis. Analysis of pedigrees has demonstrated that mother and daughter cells are not strictly equivalent: for example, they differ in their ability to undergo mating type switching (reviewed in Herskowitz and Oshima, 1981) and in the number of ARS (autonomous replication sequence) plasmids they inherit at mitosis (Murray and Szostak, 1983). The asymmetry of karmellae segregation provides another example of a distinction between the newly formed daughter and the mother cell that gave rise to it. At mitosis, karmellae remain associated with the mother cell nucleus, whereas the daughter cell inherits an unelaborated nuclear envelope. Thus, karmellae either impose asymmetric properties on the nuclear envelope, or reveal asymmetric properties of the nuclear envelope that are not otherwise apparent. This asymmetry may be established early in the cell cycle, since the akarmellar region is always oriented toward the site of bud emergence in a dividing cell. However, the akarmellar region is not consistently oriented with respect to the bud scars of previous divisions and can be found as much as 180° from its original orientation toward the bud. Therefore, in order to reorient the akarmellar region to perpetuate the axial budding pattern typical of haploid cells, either the entire nucleus must be able to rotate within the cytoplasm or the nuclear envelope must slide around the nucleoplasm to a new position after cytokinesis and septation.

HMG-CoA reductase is an integral membrane protein of the endoplasmic reticulum in mammalian cells (Chin et al., 1982, 1984; Orci et al., 1984; Liscum et al., 1985), and is likely to be the same in yeast. Karmellae formation occurs when the level of HMG1 protein is elevated only ~10-fold. Even at this level of overproduction, the protein is of low abundance, and can be detected only by immunoblotting, not directly on Coomassie Blue–stained gels. Why should modest levels of overproduction of an ER protein result in amplification of membranes associated with the nucleus? Insight into this question comes from kinetic studies of crystalloid ER formation in the mammalian UT-1 cell line. Although constitutively high levels of HMG-CoA reductase cause formation of crystalloid ER, induction of HMG-CoA reductase overproduction initially results in patches of folded membranes on the nuclear surface (Pathak et al., 1986). These patches contain HMG-CoA reductase and undergo a structural transition into crystalloid ER at later times after induction of HMG-CoA reductase synthesis. This process suggests that HMG-CoA reductase is localized in nuclear-associated membranes that will differentiate into the ER and may indicate that the ER is derived from the outer membrane of the nuclear envelope in normal cells.

In yeast, the HMG1 isozyme of HMG-CoA reductase may be initially inserted into ER membranes that are continuous with the nuclear envelope. If this membrane undergoes a subsequent transition into a mature ER morphology, then karmellae formation would occur when the rate of membrane proliferation induced by HMG-CoA reductase overproduction exceeds the rate of membrane transition or maturation. By this model, karmellae might not be induced by overproduction of the HMG2 isozyme because this isozyme is inserted into ER membranes that had already fully matured from the nuclear envelope. The different consequences of overproduction of the two isozymes would thus be directly attributed to differences in their sites of membrane insertion. In fact, precedent exists for the assembly of different membrane structures as a result of the overproduction of different

membrane proteins. The structure of ER assembled in mammalian cells in response to phenobarbital-induction of cytochrome P_{450} oxidases is qualitatively different from the crystalloid ER structure induced by HMG-CoA reductase overproduction.

Since intermediates resembling karmellae are observed in UT-1 cells during the assembly of crystalloid ER, it is unclear why yeast do not form crystalloid ER even at the highest levels of overproduction of the HMG1 isozyme. It may be significant that crystalloid ER formation occurs naturally in some mammalian tissues, which have a high rate of biosynthesis, such as the adrenal medulla (Black, 1972). The ability to form crystalloid ER may require specialized, tissue-specific factors that yeast lacks.

It might be imagined that the membrane proliferation induced by HMG-CoA reductase overproduction results from a comcomitant increase in sterol levels within the cell, since this enzyme is rate-limiting for sterol synthesis. Thus, rather than synthesizing additional membranes to accommodate the overproduced protein itself, the cell might produce additional membranes to incorporate excess sterols. This is clearly not the case in mammalian cells, since crystalloid ER formation does not occur when the catalytic domain alone is overproduced (Gil et al., 1985; Jingami et al., 1987). We think it likely that similar results will be demonstrated in yeast cells. In fact, no increase in sterol levels is observed in yeast cells that overproduce the HMG1 isozyme 10-fold, indicating that mechanisms exist to prevent sterol accumulation (Bard, M., and J. Rine, unpublished observations).

The mechanism of turnover of ER membrane proteins is unknown, although in mammalian cells the half-life of HMG-CoA reductase is responsive to cholesterol levels within the cell (Luskey et al., 1983; Faust et al., 1982; Edwards et al., 1983; Chin et al., 1985). Ultrastructural features and preliminary examination of the kinetics of karmellae assembly indicate that karmellar membranes themselves are undergoing active turnover. Ribbons of karmellae were often seen extending away from the nucleus into the cytoplasm. By analyzing serial sections of these cells, the ribbons were shown to be folds of membrane layers still associated with the nucleus at other planes of section. The events that cause some portions of karmellae to detach from the nuclear envelope and extend into the cytoplasm are not resolved. We speculate that the detachment of karmellae may represent intermediates in the normal process of membrane turnover that are difficult to detect in cells lacking karmellae. In addition, the appearance of karmellae-like membranes within the vacuole of cells with the highest levels of HMG1 overproduction raises the possibility that the vacuole has a role in ER protein turnover. In mammalian cells, the lysosome has been observed to phagocytose other organelles. Perhaps the yeast vacuole has similar capabilities.

Overproduction of the HMG2 isozyme was never observed to result in karmellae formation. We cannot exclude the possibility that the level of overproduction of the HMG2 isozyme never reached some critical threshold for karmellae formation. However, the formation of the qualitatively unique membrane stacks in HMG2-overproducing cells (Fig. 8), which were never observed in cells that overproduced the HMG1 isozyme, argues that karmellae formation is associated with some feature of the HMG1 isozyme that is not present in the HMG2 isozyme. In contrast, overproduction of the mammalian protein in yeast does induce karmellae assembly (Wright, R., and J. Rine, unpublished results). Thus, even though the membrane-bound regions of HMG1 and HMG2 proteins share ~50% sequence similarity and neither displays sequence similarity to the corresponding region of the mammalian protein (Basson, M., M. Thorsness, and J. Rine, unpublished results), both the HMG1 and the mammalian proteins elicit karmellae formation, whereas the HMG2 protein does not. The feature of the membrane-bound domains of the HMG1 and mammalian proteins that specifies karmellae formation may reflect a structural property that does not require primary sequence conservation.

Karmellae bear striking morphological similarity to naturally ocurring lamellar membrane stacks, such as the membrane disks in the outer segment of vertebrate rods and cones and the myelin sheath that encircles vertebrate axons. In light of yeast's amenability to molecular analysis, biochemical and kinetic studies aimed at understanding the processes that produce karmellae could yield important insights into the general phenomenon of membrane synthesis and assembly.

We gratefully acknowledge the support and advice of Alice Taylor and Daniela Brada regarding the electron microscopy. We also thank the members of our lab for many fruitful and stimulating discussions. Special thanks are extended to Mary Thorsness and Lorraine Pillus for their critical reading of the manuscript and helpful comments. We also wish to thank the anonymous reviewers of this manuscript for helpful suggestions.

This work was supported by grants from the California Biotechnology and Research Education Program and from the American Cancer Society to R. Wright, by a California Regents Fellowship to M. Basson, and by grants from the National Institutes of Health to J. Rine.

Received for publication 13 November 1987, and in revised form 24 March 1988.

References

Adams, A., and J. Pringle. 1984. Relationship of actin and tubulin to bud growth in wild type and morphogenetic mutant *Saccharomyces cerevisiae*. *J. Cell Biol.* 98:934–945.

Anderson, R. G. W., L. Orci, M. S. Brown, L. M. Garcia-Segura, and J. L. Goldstein. 1983. Ultrastructural analysis of crystalloid endoplasmic reticulum in UT-1 cells and its disappearance in response to cholesterol. *J. Cell Sci.* 63:1–20.

Basson, M. E., M. Thorsness, and J. Rine. 1986. *Saccharomyces cerevisiae* contains two functional genes encoding 3-hydroxy-3-methylglutaryl coenzyme A reductase. *Proc. Natl. Acad. Sci. USA.* 83:5563–5567.

Black, V. H. 1972. The development of smooth-surfaced endoplasmic reticulum in adrenal cortical cells of fetal guinea pigs. *Am. J. Anat.* 135:381–418.

Bolender, R. P., and E. R. Weibel. 1973. A morphometric study of the removal of phenobarbital-induced membranes from hepatocytes after cessation of treatment. *J. Cell Biol.* 56:746–761.

Bolivar, F., R. L. Rodriguez, R. J. Greene, M. C. Betlach, H. L. Heyneker, H. W. Boyer, J. H. Crosa, and S. Falkow. 1977. Construction and characterization of new cloning vehicles. II. A multipurpose cloning system. *Gene.* 2:95–113.

Brown, M. S., and J. L. Goldstein. 1980. Multivalent feedback regulation of HMG CoA reductase, a control mechanism coordinating isoprenoid synthesis and cell growth. *J. Lipid Res.* 21:505–517.

Brown, M. S., and R. D. Simoni. 1984. Biogenesis of 3-hydroxy-3-methylglutaryl-coenzyme A reductase, an integral glycoprotein of the endoplasmic reticulum. *Proc. Natl. Acad. Sci. USA.* 81:1674–1678.

Burnette, W. N. 1981. "Western blotting": electrophoretic transfer of proteins from sodium dodecyl sulfate-polyacrylamide gels to unmodified nitrocellulose and radiographic detection with antibody and radioiodinated Protein A. *Anal. Biochem.* 112:195–203.

Chin, D. J., G. Gil, J. R. Faust, J. L. Goldstein, M. S. Brown, and K. L. Luskey. 1985. Sterols accelerate degradation of hamster 3-hydroxy-3-methylglutaryl Coenzyme A reductase encoded by a constitutively expressed cDNA. *Mol. Cell. Biol.* 5:634–641.

Chin, D. J., K. L. Luskey, R. G. W. Anderson, J. R. Faust, J. L., Goldstein, and M. S. Brown. 1982. Appearance of crystalloid endoplasmic reticulum in compactin-resistant Chinese hamster cells with a 500-fold increase in 3-hydroxy-3-methylglutaryl Coenzyme A reductase. *Proc. Natl. Acad. Sci.*

USA. 79:1185–1189.

Clarke, L., and J. Carbon. 1980. Isolation of yeast centromeres and construction of functional small circular chromosomes. *Nature (Lond.).* 287:504–509.

Edwards, P. A., S. F. Lan, R. D. Tanaka, and A. M. Fogelman. 1983. Mevalonolactone inhibits the rate of synthesis and enhances the rate of degradation of 3-Hydroxy-3-methylglutaryl coenzyme A reductase in rat hepatocytes. *J. Biol. Chem.* 258:7272–7275.

Emr, S. D., A. Vassarotti, J. Garrett, B. L. Geller, M. Takeda, and M. G. Douglas. 1986. The amino terminus of the yeast F_1-ATPase β-subunit functions as a mitochondrial import signal. *J. Cell Biol.* 102:523–533.

Fahrenbach, W. H. 1984. Continuous serial sectioning for electron microscopy. *J. Electron Microsc. Tech.* 1:387–398.

Faust, J. R., K. L. Luskey, D. J. Chin, J. L. Goldstein, and M. S. Brown. 1982. Regulation of synthesis and degradation of 3-hydroxy-3methylglutaryl-coenzyme A reductase by low density lipoprotein and 25-hydroxycholesterol in UT-1 cells. *Proc. Natl. Acad. Sci. USA.* 79:5205–5209.

Gil, G., J. R. Faust, D. J. Chin, J. L. Goldstein, and M. S. Brown. 1985. Membrane-bound domain of HMG CoA reductase is required for sterol-enhanced degradation of the enzyme. *Cell.* 41:249–258.

Hanahan, D. 1983. Studies on transformation of *Escherichia coli* with plasmids. *J. Mol. Biol.* 166:557–580.

Hayat, M. A. 1981. Principles and techniques of Electron Microscopy. Vol. 1. University Park Press, Baltimore. 323–324.

Herskowitz, I., and Y. Oshima. 1981. Control of cell type in Saccharomyces cerevisiae. *In* The Molecular Biology of the Yeast Saccharomyces: Life Cycle and Inheritance. J. N. Strathern, E. W. Jones, and J. R. Broach, editors. Cold Spring Harbor Laboratory, Cold Spring Harbor, New York. 181–209.

Jingami, H., M. S. Brown, J. L. Goldstein, R. G. W. Anderson, and K. L. Luskey. 1987. Partial deletion of membrane-bound domain of 3-hydroxy-3-methylglutaryl coenzyme A reductase eliminates sterol-enhanced degradation and prevents formation of crystalloid endoplasmic reticulum. *J. Cell Biol.* 104:1693–1704.

Johnston, M., and R. W. Davis. 1984. Sequences that regulate the divergent *GAL1-GAL10* promoter in *Saccharomyces cerevisiae. Mol. Cell. Biol.* 4:1440–1448.

Jones, A. L., and D. W. Fawcett. 1966. Hypertrophy of the agranular endoplasmic reticulum in hamster liver induced by phenobarbital (with a review of the functions of this organelle in liver). *J. Histochem. Cytochem.* 14:215–231.

Liscum, L., J. Finer-Moore, R. M. Stroud, K. L. Luskey, M. S. Brown, and J. L. Goldstein. 1985. Domain structure of 3-hydroxy-3-methylglutaryl-Coenzyme A reductase, a glycoprotein of the endoplasmic reticulum. *J. Biol. Chem.* 260:522–530.

Luskey, K. L., J. R. Faust, D. J. Chin, M. S. Brown, and J. L. Goldstein. 1983. Amplification of the gene for 3-hydroxy-3-methylglutaryl coenzyme A reductase, but not for the 53-kDa protein, in UT-1 cells. *J. Biol. Chem.* 258:8462–8469.

McDonald, K. 1984. Osmium ferricyanide fixation improves microfilament preservation and membrane visualization in a variety of animal cells. *J. Ultrastruct. Res.* 86:107–118.

Maniatis, T., E. F. Fritsch, and J. Sambrook. 1982. Molecular Cloning. Cold Spring Harbor Laboratories, Cold Spring Harbor, New York. 545 pp.

Messing, J., B. Gronenborn, B. Muller-Hill, and P. H. Hofschneider. 1977. Filamentous coliphage M13 as a cloning vehicle: Insertion of a HindIII fragment of the *lac* regulatory region in M13 replicative form *in vitro. Proc. Natl. Acad. Sci. USA.* 74:3642–3646.

Murray, A. W., and J. W. Szostak. 1983. Pedigree analysis of plasmid segregation in yeast. *Cell.* 34:961–970.

Orci, L., M. S. Brown, J. L. Goldstein, L. M. Garcia-Segura, and R. G. W. Anderson. 1984. Increase in membrane cholesterol: a possible trigger for degradation of HMG-CoA reductase and crystalloid endoplasmic reticulum in UT-1 cells. *Cell.* 36:835–845.

Pathak, R. K., K. L. Luskey, and R. G. W. Anderson. 1986. Biogenesis of the crystalloid endoplasmic reticulum in UT-1 cells: evidence that newly formed endoplasmic reticulum emerges from the nuclear envelope. *J. Cell Biol.* 102:2158–2168.

Reynolds, G. A., S. K. Basu, T. F. Osborne, D. J. Chin, G. Gil, M. S. Brown, J. L. Goldstein, and K. L. Luskey. 1984. HMG-CoA reductase: a negatively regulated gene with unusual promoter and 5′ untranslated regions. *Cell.* 38:275–285.

Rine, J., W. Hansen, E. Hardeman, and R. W. Davis. 1983. Targeted selection of recombinant clones through gene dosage effects. *Proc. Natl. Acad. Sci. USA.* 80:6750–6754.

Roth, J. 1982. The protein A-gold (pAG) technique: a qualitative and quantitative approach for antigen localization on thin sections. *In* Techniques in Immunocytochemistry. Vol. 1. G. R. Bullock and P. Petrusz, editors. Academic Press, Inc., New York. 108–133.

Ruther, U., and B. Muller-Hill. 1983. Easy identification of cDNA clones. *EMBO (Eurl. Mol. Biol. Organ.) J.* 2:1791–1794.

Spurr, A. R. 1969. A low-viscosity epoxy resin embedding medium for electron microscopy. *J. Ultrastruct. Res.* 26:31–43.

von Meyenberg, K., B. B. Jorgensen, and B. van Deurs. 1984. Physiological and morphological effects of overproduction of membrane-bound ATP synthase in *Escherichia coli* K-12. *EMBO (Eur. Mol. Biol. Organ.) J.* 3:1791–1797.

Weiner, J. H., B. D. Lemire, M. L. Elmes, R. D. Bradley, and D. G. Scraba. 1984. Overproduction of fumarate reductase in *Escherichia coli* induces a novel intracellular lipid-protein organelle. *J. Bacteriol.* 158:590–596.